Grain Boundary Segregation Behavior of Boron in Low-Alloy Steel

GENICHI SHIGESATO, TAISHI FUJISHIRO, and TAKUYA HARA

The boron concentration profiles around prior austenite grain boundaries in Fe-0.05C-0.5Mo-0.001B (mass pct) are examined using aberration-corrected STEM-EELS. In order to obtain the precise distribution of boron around the boundaries, tilt series measurements with thin specimens (<30 nm) are performed and the EEL spectra are analyzed by principal component analysis (PCA) and multivariate curve resolution (MCR). The boron concentration profile changes with the cooling rate from the solid solution temperature. The concentration at grain boundaries is maximized at a medium rate (30 °C/s), where the concentration reaches 8 at. pct, and it decreases at a larger (250 °C/s) or smaller (5 °C/s) rate. On the other hand, the boron distribution becomes wider as the cooling rate becomes smaller. The current results suggest that the boron segregation in the alloy is formed by the "non-equilibrium segregation mechanism."

DOI: 10.1007/s11661-013-2155-3

I. INTRODUCTION

SINCE boron highly improves hardenability of steel in a small amount, boron addition is a desirable method for producing high-strength steel products without much alloying of expensive elements. However, careful attention to the production process is required to control the boron effect on hardenability because it is quite sensitive to the form of boron. It is widely accepted that solute boron segregated to austenite grain boundaries retards the nucleation of allotriomorphic ferrite on austenite grain boundaries, resulting in the improvement of hardenability.[1–3] It has also been reported that boron can easily lose its potency with precipitation.[1,4] Excessive addition of boron leads to precipitation of borocarbides and/or boron nitrides; as a result, boron becomes ineffective. Therefore, for controlling the effect of boron, it is essential to understand the behavior of boron: the change of the form and quantity on the austenite grain boundaries with the chemical compositions of the steel and heat treatment conditions.

The segregation of solute boron to austenite grain boundaries is considered to occur by two different mechanisms: equilibrium and non-equilibrium segregation. These mechanisms show different dependences of the solid solution temperature and cooling rate. According to the equilibrium segregation mechanism, the concentration of solute atoms at grain boundaries decreases exponentially as the solid solution temperature increases.[5] On the other hand, the non-equilibrium segregation mechanism, in which the segregation is formed by vacancy-solute atom pairs migrating to grain boundaries during cooling, suggests that the quantity of segregation depends on the difference between the solid solution temperature and the aging temperature. In the case that the aging temperature is the same, the amount of solute atoms segregating to grain boundaries increases as the solid solution temperature increases in opposition to the trend shown by the equilibrium segregation.[6–10]

From a qualitative perspective, non-equilibrium segregation is believed to be dominant in the conventional heat treatment conditions for steel plates.[7–13] However, the quantitative understanding of boron segregation behavior is still difficult because the two different segregation mechanisms take place simultaneously.

The authors have been developed the quantitative measurement technique for the boron concentration around austenite grain boundaries by using aberration-corrected scanning transmission electron microscopy.[14] In the present work, the behavior of boron segregation to austenite grain boundaries in low-alloy steel has been studied using the technique. The boron concentration profiles with different cooling rates have been measured and then the change of the concentration profile was discussed based on the non-equilibrium segregation theory.

II. EXPERIMENTS

A. *Materials*

A steel ingot containing about 0.001 mass pct boron was made by a vacuum melt furnace. The chemical composition is listed in Table I. The ingot was hot rolled to a thickness of 10 mm. The finishing temperature of the hot rolling was about 1223 K (950 °C). Samples for heat treatment whose dimensions were 3 mm in diameter by 10 mm in length were machined from the hot-rolled bar. The samples were heated at 1473 K (1200 °C)

GENICHI SHIGESATO, Chief Researcher, is with the Advanced Technology Research Laboratories, Nippon Steel & Sumitomo Metal Corporation, 20-1 Shintomi, Futtsu, Chiba 293-8511, Japan. Contact e-mail: shigesato.59d.genichi@jp.nssmc.com TAISHI FUJISHIRO, Researcher, and TAKUYA HARA, Chief Researcher, are with the Steel Research Laboratories, Nippon Steel & Sumitomo Metal Corporation.

Manuscript submitted May 13, 2013.
Article published online January 6, 2014

Table I. Chemical Composition of the Alloy (mass pct)

C	Mn	S	Ni	Mo	Ti	Al	N	B
0.05	1.50	0.0005	30	0.5	0.006	0.03	0.0015	0.0011

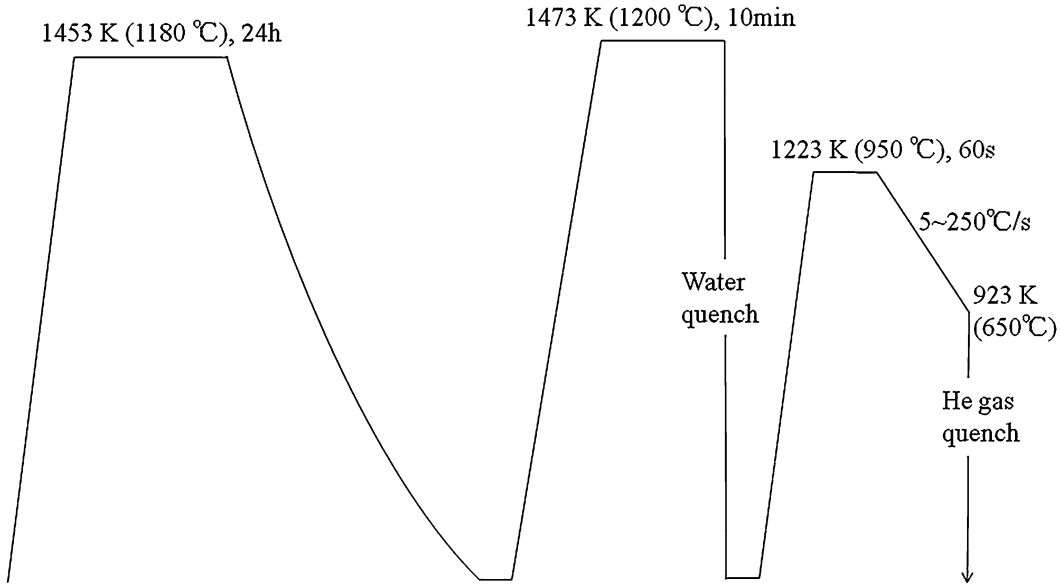

Fig. 1—Heat treatment conditions.

for 24 hours in Ar atmosphere for homogenization treatment and cooled down to room temperature in the furnace. Thermocouples were attached to the sample surface at the middle of the length after homogenization treatment. Then, the samples were reheated to 1453 K (1180 °C) for 10 minutes in Ar atmosphere for dissolving boron precipitates which were formed during cooling after the homogenization treatment and quenched by helium gas blowing. Finally, they were heated at 1223 K (950 °C) for 1 minute, cooled down to 923 K (650 °C) by three different cooling rates, 5, 30, and 250 °C/s, and then quenched by helium gas blowing. The temperatures for the solid solution treatment and the final heat treatment were measured by thermocouples attached to the samples. The heat treatment conditions are shown in Figure 1.

B. *Specimens for Microstructure Observation and EELS Analysis*

The heat-treated samples were cut in two and, the cross sections were polished mechanically and then electropolished to observe the microstructure. The microstructure was observed and analyzed using scanning electron microscopy (SEM) and electron backscatter diffraction (EBSD) to identify prior austenite grain boundaries.[14]

The specimens for scanning transmission electron microscopy (STEM) observation and electron energy loss spectroscopy (EELS) analysis were prepared by the focused ion beam (FIB) lift-out method. The blocks containing prior austenite grain boundaries, whose dimensions were about 10 μm by 10 μm by 3 μm, were picked out on semicircular Mo sheets. The picked specimens were thinned by FIB (Quanta 3D FEG) to a thickness of about 70 nm and then thinned by Ar ion milling to about 30 nm. The specimen thicknesses were measured using EEL spectra.[14] In the FIB fabrication process, a 30-kV Ga ion beam was used when the specimen thickness was larger than about 100 nm and the acceleration voltage was reduced gradually to 5 kV for thinning to about 70 nm. For Ar ion milling, the acceleration voltage of Ar ion beam was 1 kV at the beginning and then lowered gradually. The final acceleration voltage was 300 V. This procedure was adopted in order to obtain very thin and damage-less specimens.

C. *STEM Observation and EELS Analysis*

The STEM observation of prior austenite grain boundaries and the analysis of boron around the grain boundaries were performed with aberration-corrected STEM (Titan^3 80-300). The acceleration voltage used for the STEM observation and EELS analysis was 300 kV. Electron energy loss spectra were obtained along lines across the prior austenite grain boundaries. The scanning step of the line analysis was 0.1 nm. The accumulation time for one spectrum was 4 seconds. The convergence angle of the electron probe was about 18 mrad and the collection angle for the EELS detector was about 15 mrad.

III. QUANTITATIVE MEASUREMENT TECHNIQUE FOR BORON CONCENTRATION PROFILE AROUND GRAIN BOUNDARIES

The following points should be considered for the quantitative analysis of grain boundary segregation using EELS. The details of the measurement technique are described in Reference 14.

A. *Specimen Thickness*

The specimen thickness t is important for reducing the broadening of electron beam and plural scattering. The electron beam spreads with t, so that spatial resolution of analysis degrades with t. The plural scattering rate also increases with t. Plural scattering results in lowering the jump ratio of the core loss edges in the EEL spectrum and makes it difficult to detect the signal of elements in small quantities. Thus, the thinner the specimen, the better the resolution and sensitivity in EELS analysis. As discussed in the previous paper,[14] the degradation of spatial resolution of EELS analysis by beam broadening would be quite small when $t < 30$ nm for the acceleration voltage of 300 kV. In addition, the plural scattering rate is also considered to be quite small in this condition since the relative thickness t/λ_i is small enough (<0.4). For these reasons, the EELS measurements were performed at the regions where specimen thickness was about 20 to 30 nm. The thickness was examined by the log ratio method.[14,15]

B. *The Inclination of Grain Boundary*

In order to obtain the concentration profile of elements against the distance from the boundary accurately, the boundary plane must be parallel to the incident electron beam direction. If the boundary plane is inclined from the direction of electron beam, the spatial resolution of analysis will degrade. As discussed in Reference 14, the inclination should be reduced below 1 deg for keeping a good spatial resolution when the specimen thickness is 30 nm. It is, however, difficult to judge from the image of a grain boundary whether it is parallel to the electron beam direction with a precision of less than 1 degree. In order to minimize the effect of the grain boundary inclination, concentration profiles were collected as a tilt series with the step of 0.5 deg. The details were described in Reference 14.

C. *Analysis of EEL Spectra*

The analysis procedures of EEL spectra can cause significant deviation in the results of the concentration of elements. The most important process for the boron quantification is the extraction of the signal of boron from the spectra. The determination of the background shape and subtraction of the background are very sensitive processes in a relatively low-loss energy range such as the boron K edge (B–K edge) because the background shape is quite steep in the region.

In the usual manner, the background fitting is performed in a pre-edge region by using a certain background model. The power law is widely used as the model. However, the background curve calculated by the power law does not fit in a wide energy range.[15–17] Especially for a low-loss energy region, the background curve calculated by the model varies drastically with the fitting conditions: the width and the position of the fitting window. The variation of the background curve results in marked errors of the core loss intensity and the concentration of the element.

In the previous study,[14] principal component analysis (PCA) was used for the extraction of the core loss intensity. PCA is a powerful statistical tool to decompose the spectra into the components corresponding to the background, signals, and noise.[18] Thus, it is very effective to extract the signals of trace elements from EEL spectra and recognize the trend of signal intensities.[14,18,19] To quantify their concentration by using the results of PCA, however, extra attention is required.[19] For quantitative analysis, another analytical method such as multivariate curve resolution (MCR) should be used together with PCA.[20]

In the current study, a combination of PCA and MCR was adopted. The analysis procedures are summarized as below. First, a set of spectra was decomposed into the principal components (PC1, PC2, PC3…) by PCA. The noise components of which contribution rates were much smaller than those of the background and signals were removed. A new set of spectra was reconstructed with components other than the noise components. Secondly, the spectra were decomposed into the background curve and the boron signal by MCR using the first and second principle components (PC1 and PC2) as the initial functions. MCR was conducted by the alternative least square (ALS) method.[21,22]

IV. RESULTS

An example of the microstructure observed by STEM is shown in Figure 2. An apparent difference in the microstructure was not recognized among the materials of different cooling rates. No precipitate was found in all materials. Thus, it seemed that the amount of boron precipitation was little even if precipitation occurred and the majority of boron was in solid solution. However, it is not clear whether precipitation occurred or not because the specimen size was very small, typically 5 μm by 5 μm, and the observed area was limited. Especially in the steel cooled at the 5 °C/s, boron might start to precipitate.

Typical boron concentration profiles measured at prior austenite grain boundaries of the specimens cooled at 5, 30, and 250 °C/s are shown in Figure 3. The results of the measurements are summarized in Table II. The boron concentration at grain boundaries was maximized when the cooling rate was 30 °C/s. The boron concentration reached about 8 at. pct at the cooling rate. When the specimens were cooled either faster or slower, the concentration at grain boundaries reduced. On the other hand, the width of the boron concentration profile increased when the cooling rate decreased. Particularly

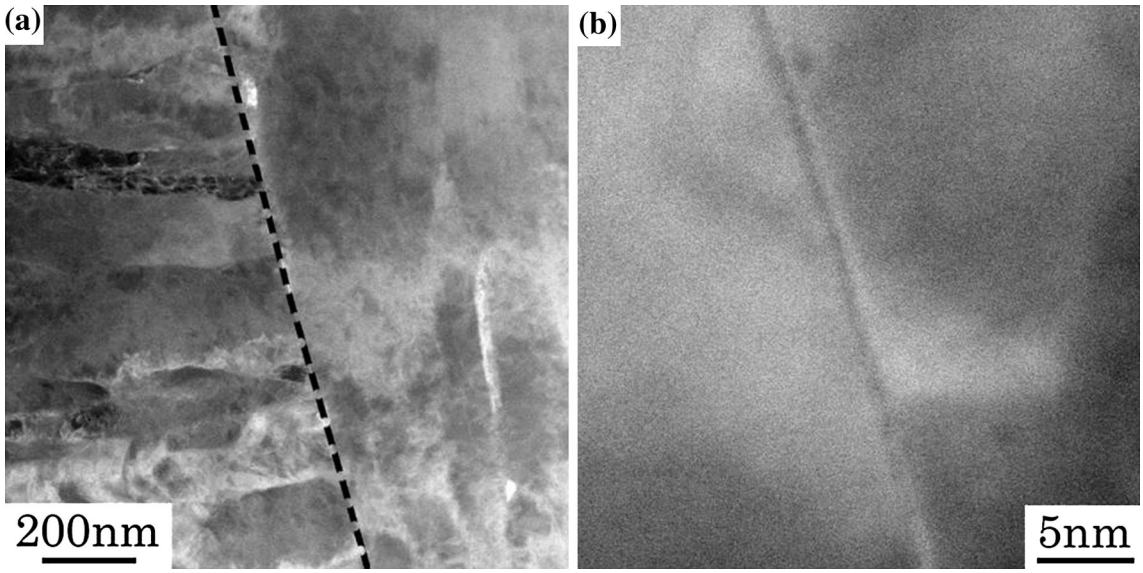

Fig. 2—Annular dark-field STEM images of the steel cooled at 30 °C/s. (*a*) A prior austenite grain boundary is indicated by the dashed line, (*b*) a magnified image of the boundary.

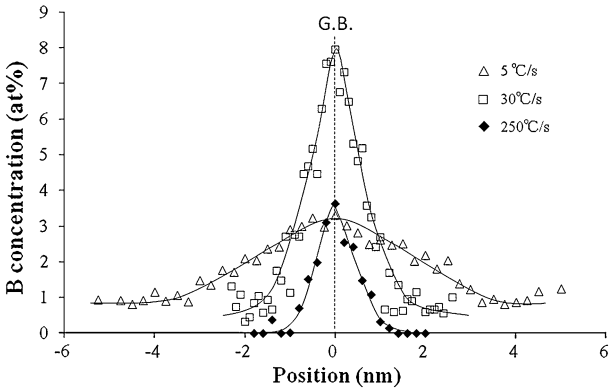

Fig. 3—Typical boron concentration profiles around prior austenite grain boundaries in the alloys cooled at 5, 30, and 250 °C/s.

when the cooling rate was 5 °C/s, the concentration profile significantly broadened.

For describing the amount of segregation, it is effective to calculate the interfacial excess of solute atoms. In the current study, the interfacial excess of boron, Γ (atoms/nm^2), was defined as the number of excess atoms in the volume created by unit area of an interface and a length perpendicular to the area (Figure 4).

$$\Gamma = N_V \int_{-l}^{l} (c - c_0) \mathrm{d}x, \qquad [1]$$

where N_V is the total number of atoms per unit volume (nm^{-3}), c is the concentration of boron in the vicinity of the interface, and c_0 is the concentration of boron in the matrix. Although the length l should be longer than the width of segregation, it was 5, 2.5, and 2.5 nm for the results of 5, 30, and 250 °C/s, respectively, because of the limited experimental data. The concentration of the matrix c_0 was set to be null since the boron content of the material was only about 10 ppm, which is much smaller than the detection limit of EELS. Boron concentration profiles were measured at several grain boundaries for each cooling condition. The results are summarized in Table II.

V. DISCUSSION

A. *Cooling Rate Dependence of Segregation*

The change of the boron concentration profile with the cooling rate can be qualitatively explained by the "non-equilibrium segregation" mechanism.

In this mechanism, segregation is formed by vacancy-solute complexes migrating to grain boundaries. When the material is cooled through a wide temperature range, the equilibrium concentration of vacancies significantly decreases. Excess vacancies formed by the rapid cooling migrate to grain boundaries and annihilate, that is, grain boundaries act as a vacancy sink. If there is an attractive interaction between vacancies and solute atoms, a proportion of the vacancies and solute atoms make vacancy-solute complexes and these complexes also diffuse to grain boundaries; as a result, segregation of solute atoms is formed around grain boundaries.

The detailed process of the non-equilibrium segregation was discussed by Faulkner[7] and Xu.[8,23–25] They introduced the critical time (t_c) and the effective time (t_e), by which the non-equilibrium segregation was divided into two processes, segregation and desegregation processes. When t_e is shorter than t_c, the segregation process takes place, where the solute concentration at grain boundaries is increasing. The concentration at grain boundaries reaches the maximum when t_e is equal to t_c. After t_e exceeds t_c, the desegregation process takes place and the concentration at the grain boundaries is decreasing.

Table II. Summary of the Results of the Boron Concentration Profile Measurements

	250 °C/s	30 °C/s	5 °C/s
Interfacial excess (atoms/nm^2)	4.0 (σ = 0.71)	11.9 (σ = l.l)	10.9 (σ = 0.76)
Concentration at G.B. (at. pct)	3.8 (σ = 0.24)	8.9 (σ = 1.00)	3.6 (σ = 0.50)
FWHM of concentration profile (nm)	0.93 (σ = 0.11)	1.2 (σ = 0.05)	4.6 (σ = 0.32)

The average values and standard deviations (σ) of the interfacial excess, concentration at grain boundaries, and the full width at half maximum (FWHM) are shown. The numbers of measured grain boundaries were 3, 4, and 3 for 250, 30, and 5 °C/s, respectively.

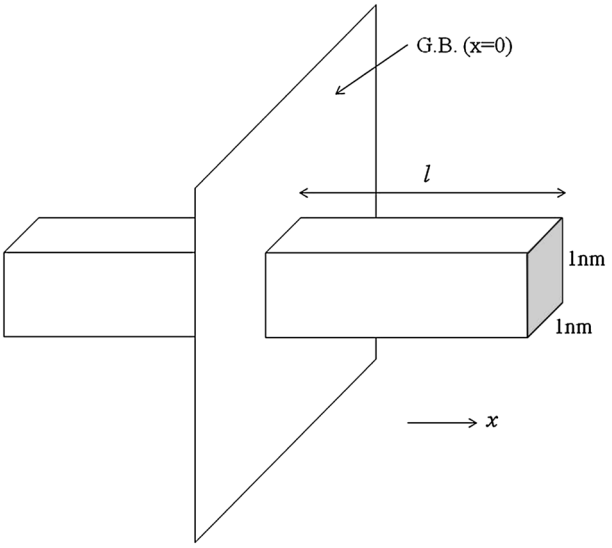

Fig. 4—Schematic figure of a grain boundary and the column for counting the interfacial excess of solute.

When a material is cooled from the solution treatment temperature (T_0) to the isothermal annealing temperature (T_1) and the cooling is supposed to be rapid enough to neglect the diffusion during the cooling, the critical time after which desegregation begins, t_c, is determined by the diffusion rate of the vacancy-solute complex toward a grain boundary and the diffusion rate of solute away from the grain boundary[23]

$$t_c = \frac{d^2 \ln(D_c/D_i)}{4\delta(D_c - D_i)}, \quad [2]$$

where D_c is the diffusion coefficient of the complex, D_i is the diffusion coefficient of the solute, d is the grain size, and δ is a constant. Inserting the parameters listed in Table III, t_c for the current experiment is obtained as 4.8 seconds.

For continuous cooling, the effective time for annealing can be evaluated by decomposing the cooling curve into small steps of isothermal annealing for Δt and rapid cooling ΔT.

$$t_e = \sum_{i=1}^{n} \Delta t_i \exp\left\{\frac{-E_A \Delta T_i}{k T_0 T_i}\right\}, \quad [3]$$

where E_A is the average activation energy for diffusion of complexes and impurities, and k is the Boltzmann's constant. Figure 5 shows t_e calculated for continuous cooling from T_0 [1223 K (950 °C)] to T_1 [923 K (650 °C)] with various cooling rates. The parameters used in the calculation are listed Table III. As discussed in Reference 23, the smaller the $\Delta T \Delta t$, the more accurate the calculated t_e. In this study, the calculation was conducted with $\Delta T \Delta t = 1$ for all cooling rates.

Table III. Data Used for the Current Calculation

D_i (m^2 s^{-1})	$2 \times 10^{-7}\exp(-0.91/kT)$	[26]
D_c (m^2 s^{-1})	$5 \times 10^{-5}\exp(-0.91/kT)$	[26]
d (nm)	30	
δ	0.48	[25]
E_f	1 4	[26]
E_A	0.91	[26]
E_B	0.5	[26]

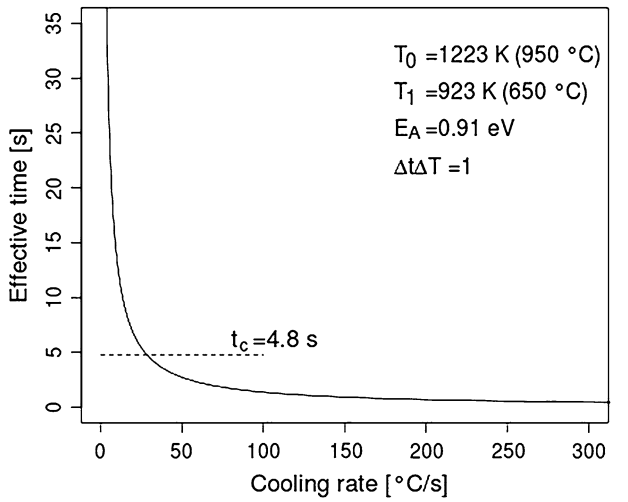

Fig. 5—Effective time calculated for various cooling rates. The critical time calculated for the current experimental condition is also indicated.

In Figure 5, the critical time t_c is also indicated, at which transition from segregation to desegregation occurs. The cooling rates of the current experiment were in different stages. Apparently, the cooling rate of 250 °C/s is in the region of segregation and 5 °C/s is in the region of desegregation. The cooling rate of 30 °C/s is almost identical to t_c. Therefore, the concentration at the grain boundary should be maximized when the cooling rate is 30 °C/s.

When the material is cooled much faster than t_c, the diffusion distance during cooling is small and the amount of vacancy-solute complexes migrating to grain

boundaries is limited. Thus, the boron segregation decreases as the cooling rate increases. In fact, as shown in Table II, the amount of boron segregated around grain boundaries was smaller when the cooling rate was 250 °C/s than 30 and 5 °C/s.

If the material is cooled rather slowly, on the other hand, the desegregation process occurs.[7,8,10,11] As a result, the concentration at the grain boundary when the cooling rate was 5 °C/s was smaller than when it was 30 °C/s.

The experimental results of the current study show that the width of the concentration profile increased as the cooling rate decreased. That is because boron atoms can diffuse from further as the material is cooled more slowly. In addition, desegregation can broaden the concentration profile when the cooling rate is very small. Accordingly, the boron concentration profile of 5 °C/s was much broader than those of 30 and 250 °C/s.

B. *Boron Concentration at Grain Boundary*

From a quantitative perspective, however, it is difficult to explain the current results only by the non-equilibrium segregation mechanism. As reported in Reference 23, when a material is cooled rapidly from T_0 to T_1, the maximum concentration of solute at the grain boundary by the non-equilibrium segregation mechanism, C_{gb}, is obtained as the following equation.

$$\frac{C_{gb}}{C_g} = \exp\left\{\frac{E_b - E_f}{kT_0} - \frac{E_b - E_f}{kT_1}\right\}\frac{E_b}{E_f}, \qquad [4]$$

where E_b is the formation energy of the complex, E_f is the formation energy of the vacancy, and C_g is the concentration within the grain. Using the parameters listed Table III, C_{gb} at the annealing temperature T_1 was calculated (Figure 6). As T_1 decreases, that is, the difference between T_0 and T_1 increases, C_{gb} increases, which represents one of the aspects of non-equilibrium segregation. The concentration at the grain boundary is, however, about 0.06 mass pct, which is much smaller than the measured concentration of the present study.

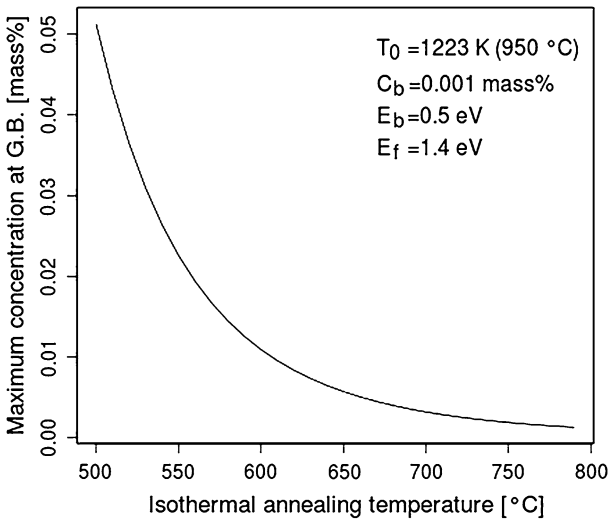

Fig. 6—The maximum concentration at a grain boundary calculated for various isothermal annealing temperatures.

Karlsson and Nordon[9] also reported the significant difference between the experimental results and the calculation of the grain boundary segregation. Karlsson measured the boron concentration at grain boundaries in austenitic stainless steel using an Atom Probe. The measured boron concentration at the grain boundary exceeded 10 at. pct, while the concentration at the grain boundary calculated by the diffusion equations based on the non-equilibrium segregation mechanism was about several hundred ppm. Xu and Song[24] also presented the calculated boron concentrations at the grain boundary, which were also much less than 1 at. pct.

The reason for the difference between the measurements and calculation is not clear at the present time. One of the reasons is attributed to the difficulty to estimate the adequate value of the parameters for the calculation, such as the binding energy of a vacancy and a solute atom and the diffusivity of the vacancy-solute complexes. Another possibility is that the mechanism may be more complicated. Although the calculation assumed only non-equilibrium segregation, it is considered that both equilibrium and non-equilibrium segregation occur simultaneously in reality. Especially when the cooling rate is small, the contribution of equilibrium segregation should be considerable. Moreover, although it was assumed that the vacancy-boron complex consisted of one vacancy and one boron atom, it could consist of plural vacancies and atoms. For the quantitative prediction of the segregation behavior, further investigation is required experimentally and theoretically.

VI. SUMMARY

The segregation behavior of boron in Fe-0.05 pct C-3 pct Ni-0.5 pct Mo-0.001 pct B alloy was investigated using aberration-corrected STEM. The results can be summarized as follow:

1. The boron concentration profile around austenite grain boundaries changed with the cooling rate from the solid solution temperature [1223 K (950 °C)]. The amount of segregation, which was estimated by the Gibbsian interfacial excess, increased when the cooling rate decreased. The concentration at grain boundaries was maximized at a medium rate (30 °C/s), where the concentration reached 8 at. pct, and it decreased when the materials were cooled more rapidly (250 °C/s) or slowly (5 °C/s). By contrast the width of the profile increased as the cooling rate decreased.
2. According to the above results, the boron segregation to austenite grain boundaries was considered to be formed by the non-equilibrium segregation mechanism.

REFERENCES

1. M. Ueno and T. Inoue: *Trans. ISIJ*, 1973, vol. 13, p. 210.
2. J.E. Morral and T.B. Cameron: *Metall. Trans.*, 1977, vol. 8, p. 1817.

3. J. Morral and T. Cameron: in *Boron in Steel*, S. Banerji and J. Morral, eds., AIME, Warrendale, 1980, pp. 19–32.
4. P. Maitrepierre, D. Thivellier, and R. Tricot: *Met. Trans. A*, 1975, vol. 6, pp. 287–301.
5. D. Mclean: *Grain-Boundaries in Metals*, Oxford University Press, Oxford, 1957.
6. T.R. Anthony: *Acta Metall.*, 1969, vol. 17, pp. 603–09.
7. R.G. Faulkner: *J. Mater. Sci.*, 1981, vol. 16, pp. 373–83.
8. T. Xu: *J. Mater. Sci.*, 1987, vol. 22, pp. 337–45.
9. L. Karlsson and H. Nordon: *Acta Metall.*, 1988, vol. 36, pp. 13–24.
10. L. Karlsson: *Acta Metall.*, 1988, vol. 36, pp. 25–34.
11. X.L. He, Y.Y. Chu, and J.J. Jonas: *Acta Metall.*, 1988, vol. 37, pp. 2905–16.
12. G. Carinci: *Appl. Surf. Sci.*, 1994, vols. 76–77, pp. 266–71.
13. M. Chapman and R. Faulkner: *Acta Metall.*, 1983, vol. 31, pp. 677–89.
14. G. Shigesato, T. Fujishiro, and T. Hara: *Mater. Sci. Eng.*, 2012, vol. A556, pp. 358–65.
15. R.F. Egerton: *Electron Energy-Loss Spectroscopy*, 2nd ed., Plenum Press, New York, 1996.
16. J. Verbeeck and S. Van Aert: *Ultramicroscopy*, 2001, vol. 101, pp. 207–24.
17. R.F. Egerton and M. Malac: *Ultramicroscopy*, 2002, vol. 92, pp. 47–56.
18. M.A. Sharaf, D.L. Illman, and B.R. Kowalski: *Chemometrics, Chemical Analysis*, John Wiley & Sons, New York, 1986, vol. 82.
19. N. Bonnet: *Ultramicroscopy*, 1999, vol. 77, pp. 97–112.
20. S. Muto, T. Yoshida, and K. Tatsumi: *Mater. Trans. JIM*, 2009, vol. 50, pp. 964–69.
21. R. Tauler, B. Kowalski, and S. Fleming: *Anal. Chem.*, 1993, vol. 65, pp. 2040–47.
22. A. de Juan, Y. Vander Heyden, R. Tauler, and D.L. Massart: *Anal. Chim. Acta*, 1997, vol. 346, pp. 307–18.
23. T. Xu: *J. Mater. Sci. Lett.*, 1988, vol. 7, pp. 241–42.
24. T. Xu and S. Song: *Acta Metall.*, 1989, vol. 37, pp. 2499–2506.
25. T. Xu and B. Cheng: *Prog. Mater Sci.*, 2004, vol. 49, pp. 109–208.
26. T.M. Williams, A.M. Stoneham, and D.R. Harries: *Met. Sci.*, 1976, vol. 10, pp. 14–19.